Cu atoms suppress misfit dislocations at the β"/Al interface in Al-Mg-Si alloys

Takeshi Saito [*,1,2], Flemming J.H. Ehlers [2,A], Williams Lefebvre [3], David Hernandez-Maldonado [3,B], Ruben Bjørge [4], Calin D. Marioara [4], Sigmund J. Andersen [4], Eva A. Mørtsell [2], Randi Holmestad [2]

[1] Hydro Aluminium, Research and Technology Development, N-6601 Sunndalsøra, Norway
[2] Department of Physics, Norwegian University of Science and Technology (NTNU), N-7491 Trondheim, Norway
[3] Université de Rouen, GPM, UMR CNRS 6634 BP 12, Avenue de l'Université, 76801 Saint Etienne du Rouvray, France
[4] SINTEF Materials and Chemistry, N-7465 Trondheim, Norway

*Corresponding author:
Email: takeshi.saito@hydro.com
Postal address: Hydro Aluminium, Research and Technology Development, Romsdalsvegen 1, 6600 Sunndalsøra, Norway

[A] Current affiliation: Université Paris Diderot, Sorbonne Paris Cité, ITODYS, UMR 7086 CNRS, 15 rue J.-A.deBaïf, 75205 Paris cedex 13, France

[B] Current affiliation:
SuperSTEM Laboratory, Daresbury, UK

Abstract

The Cu interactions with the Al-Mg-Si alloy main hardening phase β" are investigated in atomic scale, by using experimental and simulated high angle annular dark-field scanning transmission electron microscopy techniques and density functional theory calculations. Cu is located at or near the β"/Al interface, with the misfit dislocations normally observed for a precipitate of this size being absent. It is proposed that the small Cu volume is crucial to this mechanism. Present supercell based calculations cannot fully model these interactions.

Main Text

Hardness evolution under heat treatment is a topic of central interest for age-hardenable Al alloy development. An intimate connection exists between strength and solute atom nanostructures [1]. For Al-Mg-Si alloys, maximum hardness is reached through formation and growth of semi-coherent needle-shaped (β") precipitates [2, 3] possessing significant misfits with the Al matrix in the needle cross-section. For large precipitates, the misfit triggers the introduction of dislocations at the β"/Al interface. This directly influences precipitate growth, and in turn hardness evolution.

The monoclinic β" phase (Figure 1(a)) has orientation relationships with the face-centred cubic (fcc) Al matrix given as [230]Al // [100]β", [001]Al // [010]β", and [-310]Al // [001]β". Along the β" needle direction [010] β", the experimentally reported [3] lattice misfit is vanishing.

In the needle cross-section (Al // (100) and Al // (001) habit planes), it is high and positive: 5.3% and 3.8%, respectively. The interfaces are locally coherent, but with added misfit dislocations for large β" cross-sections. Experimental and theoretical studies [4-7] largely agree on a β" composition fluctuating around $Mg_5Al_2Si_4$.

While the effect of Cu on the precipitation sequence in Al-Mg-Si alloys has received considerable attention [8, 9], relatively little work has addressed Cu-β" interactions. Both atom probe tomography (APT) studies [5, 10] as well as high angle annular dark-field scanning transmission electron microscopy (HAADF-STEM) investigations combined with energy dispersive X-ray spectroscopy (EDX) [11] have shown that Cu is incorporated in β". Information on the effect of Cu on β" growth however has so far been lacking.

In this work, we present experimental support for a Cu induced modification of the β" growth path. We demonstrate that Cu binds at or near the β"/Al interface, effectively suppressing the misfit dislocations observed in its absence. Based on theoretical considerations, we propose that the origin of this mechanism is two-fold: Cu has an affinity for β" and an atomic volume significantly smaller than the Al atom it replaces. The resulting Cu induced strain relief reduces – and potentially even eliminates – the need for misfit dislocations.

Our results were achieved by comparing experimental and simulated HAADF-STEM image analysis with theoretical density functional theory (DFT) based calculations. For the analysed sample, an alloy with composition Al-0.52Mg-0.38Si-0.04Cu (at%) was prepared by extrusion from cast billets. This composition falls within the specifications of commercial 6060 Al alloys, except for the Cu addition. Other impurities are below 0.01 at%. The alloy was solution heat treated at 545°C for 5 min, kept for 30 min at room temperature and isothermally heat treated at 190°C for 300 min – a procedure inducing the peak hardness condition [12]. HAADF-STEM specimens were prepared by electropolishing with a Tenupol 5 machine (Struers). The electrolyte consisted of 1/3 HNO3 in methanol and the solution was kept at a temperature between -20°C and -35°C. All specimens were ion-milled in a precision ion polishing system (PIPS, Gatan), and subsequently plasma cleaned before HAADF-STEM imaging in order to reduce the effect of contamination, using a Model 1020 Plasma Cleaner (Fischione Instruments). The HAADF-STEM images were taken by a spherical aberration (Cs) probe-corrected JEOL ARM200F STEM with a Schottky field emitter operating at 200 kV. The probe size was 0.1 nm. The convergence semi-angle of the electron probe was 20 mrad and the collection angle of the HAADF detector was in the range of 45-150 mrad. The thickness of the specimen was estimated to about 40 nm by Gatan parallel electron energy loss spectroscopy. The HAADF-STEM technique provides atomic number contrast [13], making even minor Cu concentrations in each column distinguishable.

The combined experimental and theoretical methodology has been described in detail in Ref. [14] and references cited therein. The analysis of the experimental HAADF-STEM intensities was conducted by measurement of integrated column intensities for each column, assuming fixed column atom density. HAADF-STEM simulations were conducted using the frozen phonon multislice program provided by the QSTEM package [15]. Bulk β" and interface {-320}Al β"/Al structures were modelled, using experimentally reported [3] and DFT structural parameters, respectively. For the simulations, adjustable parameters (slice thickness, convergence semi-angle,

HAADF collector angles, frozen phonon configurations and Debye-Waller factors) defined in Ref. [14] were unaltered. The chosen Debye-Waller factor for the Cu site matched the elemental phase value at 300 K: 0.5747 Å^2 [16]. Finally, the theoretical DFT based [17, 18] studies employed Vanderbilt ultrasoft pseudopotentials [19] as implemented in the plane wave (PW) based code VASP [20, 21], with the Perdew-Wang generalized gradient approximation for the exchange-correlation energy [22]. Bulk β" and interface β"/Al structures (both habit plane interfaces) were examined, using 44 and 88 atom supercells, respectively (see section 1 of the Supplementary Material for details). Cu binding energies at the β"/Al interface were computed as the energy change upon moving this "defect" from a fcc Al 108 atom supercell to a Si3/Al site in the interface cell (and Al the other way). By comparison, the (bulk β") "replacement energies" [14] typically involve introduction of additional Al defects for the reference configurations, generally comparing the Cu introduction with the best solute atom alternative. Calculations used a 234 eV PW cut-off, with compatible Monkhorst-Pack k-point grids for the various cells ((12, 6, 14) for the conventional β" cell).

Figure 1 (b) shows an experimental HAADF-STEM image of a β" precipitate, with a colour mapping of atomic column intensities for the same system displayed in Figure 1 (c). Figure 1 (d) reveals that high intensities systematically correspond with the Si3/Al site at the interface along [230]Al. Along [-310]Al, such bright Si3/Al atomic columns are less systematic at the interface, but some are present half a unit cell into β", see Figure 1 (d). Comparing the average intensities of the Si3/Al sites at the bulk and the interface in Figure 1 (c) (see section 2 of Supplementary Materials for details), we find the latter to be higher by ~24%.

Without Cu introductions, the simulated HAADF-STEM intensities for the bulk and {-320}Al interface Si3/Al sites differ only weakly (see Figure 2). For a specimen thickness of 40 nm (which is represented by Figure 1 (b)), the interface intensities are higher by ~12% (due to the misfit strain and/or interface electronic effects [14]). Note that the intensity difference is twice as high in the experiment (~24%). It hence seems clear that a pure β"/Al interface cannot explain the observations in Figure 1. We add that no similarly bright Si3/Al interface columns were reported in recent studies of Cu-free [7, 14] Al-Mg-Si alloy systems, where the HAADF-STEM images were acquired under conditions and at specimen thicknesses similar to those of the present work.

When adding 5% Cu at the interface Si3/Al site in the HAADF-STEM simulations, however, the bulk-interface intensity difference rises to 42%. If we assume a linear variation with Cu occupancy for the intensity of Figure 2, an average 3% Cu occupancy at each Si3/Al interface site may explain Figure 1 (d). The resulting 0.15% Cu concentration in the full precipitate is very similar to the APT results (Figure 8) of Ref. [10]. We conclude that the high interface column intensities in Figure 1 (d) are likely due to Cu incorporation.

A notable feature in Figure 1 (b) is the absence of misfit dislocations at the β"/Al interface. Normally, β" precipitates of this size incorporate one or more dislocations, in response to the accumulated misfit in the cross-section (see Figure 3). Judged from the experimental analysis alone, we expect Cu to induce this misfit suppression. Additional β" precipitates were examined, see section 3 of the Supplementary Material. We found all features discussed above to be qualitatively reproduced.

Figure 4 (a) shows the calculated binding energies for Cu to selected Si3/Al sites in the β"-$Mg_5Al_2Si_4$ phase. A Cu-free precipitate and an isolated Cu atom in the Al matrix serve as the reference state. Cu clearly binds to β", weakly preferring the precipitate interior. Only at the {130}Al interface is the binding energy clearly higher.

The supercell based modelling of Figure 4 (a) has an inherent limitation [23]: the cell periodic boundary conditions truncate the strain evolution along the interface. A foreign atom added at this interface however technically interacts with the full precipitate strain field. It follows that whenever the resulting strain field modulation is noteworthy, the model scheme used above will be dissatisfactory. To our knowledge, this limitation is not commonly stressed. For the Cu-β" interactions of Figure 4 (a), this topic is likely important. Table 1 shows that the Cu volume is always markedly below the volume of the precipitate Al atom it replaces – roughly 40% for Cu in the matrix. Since β" is under significant compressive strain, the Cu incorporation definitely provides strain relief. This effect will be most pronounced in the part where the compression of the precipitate is strongest, namely at the interface.

The above consideration is qualitative in nature, reflecting our inability within DFT to optimize the system of an isolated β" precipitate of the size shown in Figure 1 (b). In the absence of such studies, we emphasize here only a few points of expected interest. First, we note that our analysis appears consistent with the observations in Figure 1 (b). Adding the presumed strain relief effect to the results of Figure 4 (a) likely stabilizes Cu incorporation at the interface along [230]Al, but presumably only serves to drive Cu towards the interface along [-310]Al. Second, we may compare our results with those obtained recently for Zn incorporation in β" [14]. According to the DFT studies, Zn behaves qualitatively like Cu, preferring a bulk β" Si3/Al site. However, unlike Cu, Zn is only weakly smaller than Al, implying little strain relief. As expected, theory shows good agreement with experiment for this case. Finally, we stress the qualitative similarities between the effect of (i) decorating the β"/Al interface with Cu on the β" side and (ii) introducing a misfit dislocation on the Al side. In both cases, the local defect may enhance the strain field perpendicular to the interface, but certainly will reduce the subsystem misfit along it.

In recent HAADF-STEM investigations [11], Cu was reported to occupy the Mg1 and the Si3/Al sites throughout the β" precipitate. To examine this issue further, we calculated a full set of replacement energies (see Ref. [14]) for Cu in β"-$Mg_{5+x}Al_{2-x}Si_4$, x = {-1, 0, 1}. The results, shown in Figure 4 (b), provide no support for Cu incorporation on the Mg1 site. We also performed additional experiments to produce smaller β" precipitates, comparable to Ref. [11]. The resulting HAADF-STEM images (examples in section 3 of the Supplementary Material) were qualitatively similar to Figure 1 (b). Incidentally, this result indicates that the Cu diffusion in β" is low, complicating the discussion of the bias in Figure 4 (a).

Our studies have stressed important experimental and theoretical aspects of how Cu interacts with β" precipitates in Al-Mg-Si alloys. Cu has a preference for the β"/Al interface vicinity, suppressing misfit dislocations stabilized in its absence. Similar to the dislocations, Cu provides strain relief (due to its small atomic volume compared to Al), explaining the substitution. Quantitative DFT calculations of this effect however are presently out of reach, with standard interface supercell studies likely failing to even predict the correct Cu location in β". We believe

all these phenomena to be of importance whenever the precipitate-matrix interface is coherent and misfit, with the attaching solute atom strongly affecting the strain field. To clarify the Cu influence on β" growth, statistical studies of β" cross-sections and aspect ratios would be of interest.

Acknowledgements

References

[1] I.J. Polmear, Mater. Forum 28 (2004) 1-14.
[2] G.A. Edwards, K. Stiller, G.L. Dunlop, M.J. Couper, Acta Mater. 46 (1998) 3893-3904.
[3] S.J. Andersen, H.W. Zandbergen, J. Jansen, C. Træholt, U. Tundal, O. Reiso, Acta Mater. 46 (1998) 3283–3298.
[4] H.S. Hasting, A.G. Frøseth, S.J. Andersen, R. Vissers, J.C. Walmsley, C.D. Marioara, F. Danoix, W. Lefebvre, R. Holmestad, J. Appl. Phys. 166 (2009) (123527-1–123527-9).
[5] S. Pogatscher, H. Antrekowitsch, H. Leiner, A.S. Sologubenko, A.S. Uggowitzer, Scr. Mater. 68 (2013) 158-161.
[6] F.J.H. Ehlers, Comput. Mater. Sci. 81 (2014) 617-629.
[7] P.H. Ninive, A. Strandlie, S. Gulbrandsen-Dahl, W. Lefebvre, C.D. Marioara, S.J. Andersen, J. Friis, R. Holmestad, O.M. Løvvik, Acta Mater. 69 (2014) 126-134.
[8] D.J. Chakrabarti, D.E. Laughlin, Prog. Mater. Sci. 49 (2004) 389-410.
[9] C.D. Marioara, S.J. Andersen, T.N. Stene, H. Hasting, J. Walmsley, A.T.J. van Helvoort, R. Holmestad, Philos. Mag. 87 (2007) 3385-3413.
[10] G. Sha, H. Möller, W.E. Stumpf, J.H. Xia, G. Govender, S.P. Ringer, Acta Mater. 60 (2012) 692-701.
[11] K. Li, A. Beche, M. Song, G. Sha, X. Lu, K. Zhang, Y. Du, S.P. Ringer, D. Schryvers, Scr. Mater. 75 (2014) 86-89.
[12] T. Saito, S. Muraishi, C.D. Marioara, S.J. Andersen, J. Røyset, R. Holmestad, Metall. Mater. Trans. A 44 (2013) 4124-4135.
[13] S.J. Pennycook, Adv. Imag. Elect. Phys. 123 (2002) 173-206.
[14] T. Saito, F.J.H. Ehlers, W. Lefebvre, D. Hernandez-Maldonado, R. Bjørge, C.D. Marioara, S.J. Andersen, R. Holmestad, Acta Mater. 78 (2014) 245-253.
[15] C.T. Koch, PhD. Thesis. Determination of core structure periodicity and point defect density along dislocations. Arizona State University, (2002).
[16] H.X. Gao, L.M. Peng, Acta Cryst. A 55 (1999) 926-932.
[17] P. Hohenberg, W. Kohn, Phys. Rev. B 136 (1964) 864-871.
[18] W. Kohn, L.J. Sham, Phys. Rev. A 140 (1965) 1133-1138.
[19] D. Vanderbilt, Phys. Rev. B 32 (1985) 8412-8415.

[20] G. Kresse, J. Hafner, Phys. Rev. B 47 (1993) 558-561.

[21] G. Kresse, J. Furthmuller, Comput. Mater. Sci. 6 (1996) 15-50.

[22] J.P. Perdew, J.A. Chevary, S.H. Vosko, K.A. Jackson, M.R. Pederson, D.J. Singh C. Fiolhais, Phys. Rev. B 46 (1992) 6671-6687.

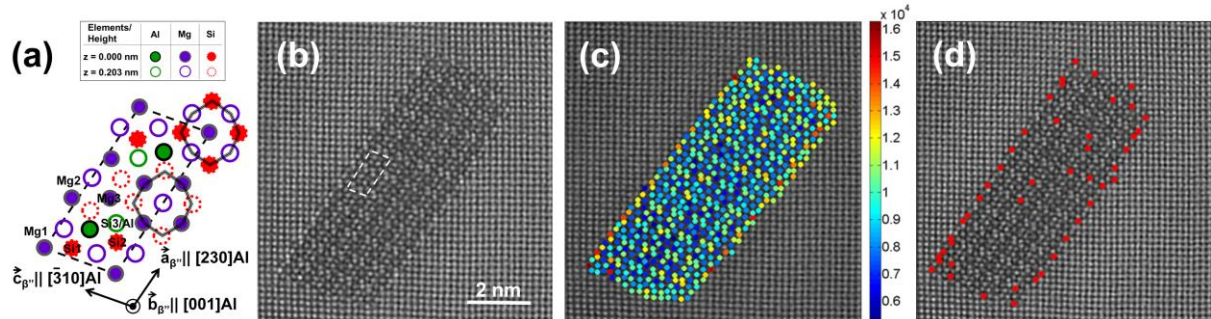[23] F.J.H. Ehlers, R. Holmestad, Comput. Mater. Sci. 72 (2013) 146-157.

Figure 1 Experimental HAADF-STEM analysis of a β" precipitate. (a) The β" unit cell (dashed lines) viewed along the monoclinic axis. The characteristic 4-fold atomic coordination around the Mg1 site (triple solid line) is easily visible in the experimental image. (b) Fast Fourier transform (FFT) filtered HAADF-STEM image of a β" cross-section, taken along <001>Al. The noise reducing FFT filtering used a circular band pass mask, removing all periods shorter than 0.15 nm. A β" unit cell has been highlighted. (c) Colour mapping of the integrated intensity (arbitrary units) for selected sites from (b). (d) Atomic columns for selected sites (red dots) having intensities greater than 12000 a.u. from (c).
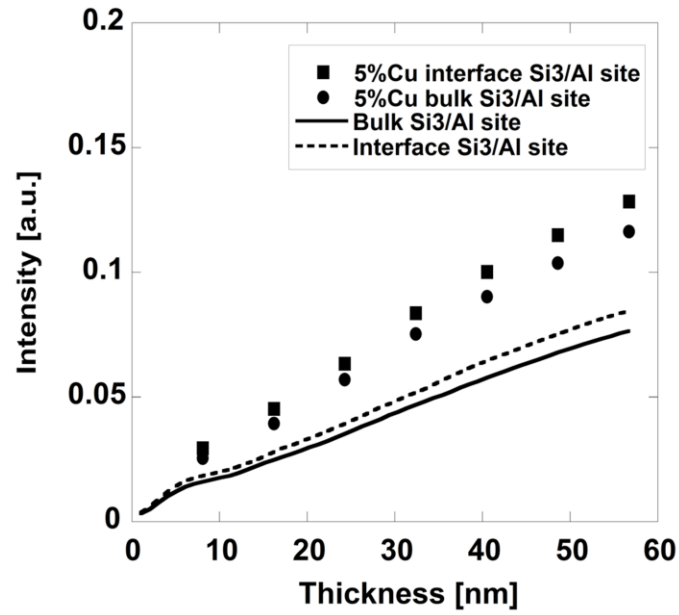
Figure 2 Simulated HAADF-STEM intensities for bulk and {-320}Al interface β"-Mg$_5$Al$_2$Si$_4$ Si3/Al site atomic columns, as a function of specimen thickness. For the replacement of 5% Al with Cu, an even distribution along the electron beam direction was assumed, see e.g. Ref. [14].
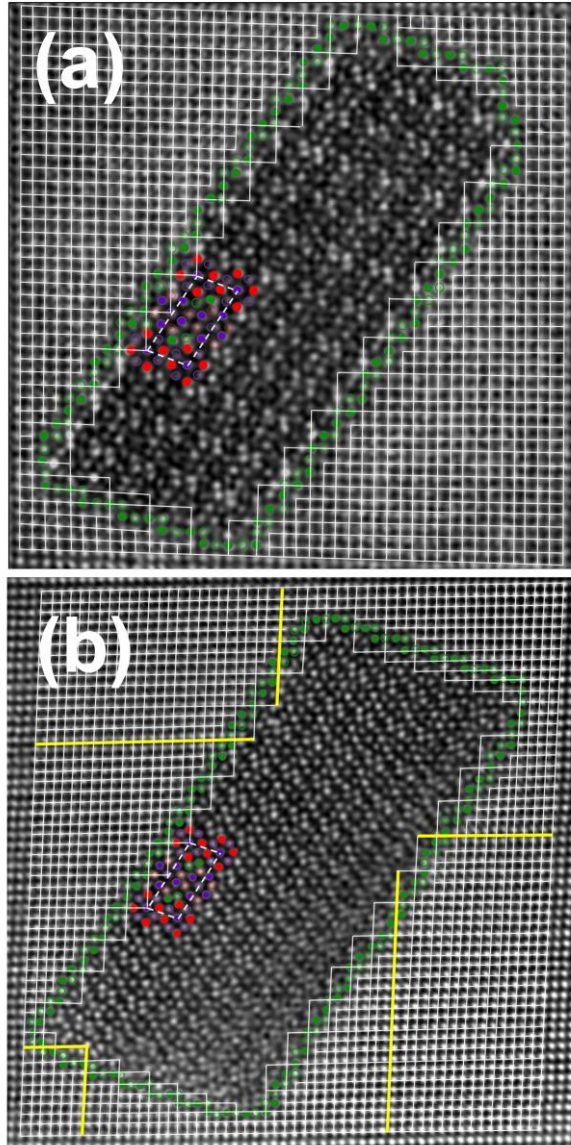
Figure 3 (a) The β" precipitate from Figure 1 (b) (5.5×4 (a×c) unit cell cross-section), with added overlay. A β" unit cell is represented as dashed lines, with atom types highlighted as in Figure 1 (a). White parallel solid lines track {100}Al planes, separated by 2.025Å. These are led periodically into the precipitate, terminating at identical atom sites (Mg1) in β", emphasizing the full coherence with the Al matrix (no interface dislocations). For comparison, (b) shows a β" precipitate (6×6 unit cell cross-section) for a Cu-free alloy with an otherwise similar composition and acquired at a similar HAADF-STEM condition. This precipitate hosts clear misfit dislocations (yellow solid lines).
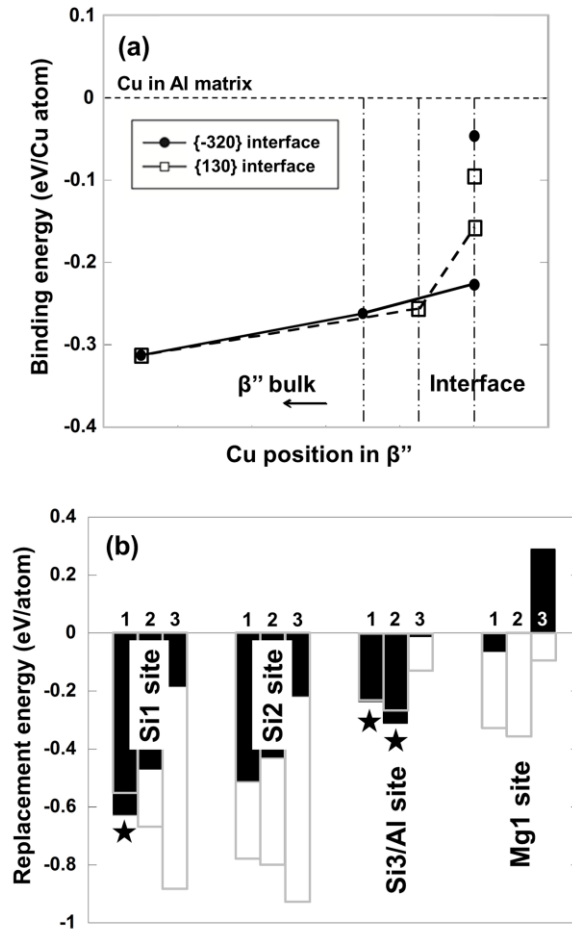
Figure 4 (a) Computational (DFT) studies of Cu-β" interactions. (a) Cu binding energies in β"-Mg$_5$Al$_2$Si$_4$ for selected Si3/Al site positions. Right vertical line: interface. Other vertical lines: movement into β" bulk by half a unit cell (squares) and one unit cell (circles) along {-320} and {130} interfaces, respectively. (b) Replacement energies (see Ref. [14]) for Cu (black bars) and alternative solute atoms Mg/Si (white bars) on selected sites in three different β" configurations, 1: Mg$_4$Al$_3$Si$_4$, 2: Mg$_5$Al$_2$Si$_4$ and 3: Mg$_6$AlSi$_4$. Cu hardly binds at the excluded sites Mg2, Mg3. The black stars show favourable sites for Cu incorporations at the corresponding β" configurations.

Table 1 Calculated (DFT) Cu-Al volume differences $\Delta V_{Al \rightarrow Cu: X}$, for selected systems X. The calculated Al volume in fcc Al is 16.5Å^3.

System X	$\Delta V_{Al \rightarrow Cu: X}$ [Å^3/atom]
fcc Al	-6.8
β"-Mg$_5$Al$_2$Si$_4$	-8.3
β"/Al, along [-310]Al	-7.5
β"/Al, along [230]Al	-6.4